

PCM, ETS-NOCV, and CDA investigations of interactions of a Cycloplatinated Thiosemicarbazone as antiparasitic and antitumor agents with C₂₀ nano-cage

Amir Solgi ¹, Reza Ghiasi* ², Sahar Baniyaghoob ¹

¹ Department of Chemistry, Science and Research Branch, Islamic Azad University, Tehran, Iran

² Department of Chemistry, East Tehran Branch, Islamic Azad University, Tehran, Iran

Received 28 March 2023,

revised 26 April 2023,

accepted 03 May 2023,

available online 18 May 2023

Abstract

In this work, we reported a computational investigation on the interaction between a cycloplatinated thiosemicarbazone (CT) as antiparasitic and antitumor agents with C₂₀ molecule. The solvent impacts were considered by the SCRF based on PCM. The relationships of solvation energies, interaction energy, dipole moment, and N-H stretching frequencies ($\nu(\text{NH})$) values with *modified-Buckingham* function were illustrated. ETS-NOCV, CDA, and EDA results provided valuable understanding into the interaction between two fragments.

Keywords: Cycloplatinated Thiosemicarbazones; C20 Molecule; Charge Decomposition Analysis (CDA); Energy Decomposition Analysis (EDA); Extended Transition State-Natural Orbitals for Chemical Valence (ETS-NOCV); Polarizable Continuum Model (PCM).

How to cite this article

Solgi A., Ghiasi R., Baniyaghoob S., PCM, ETS-NOCV, and CDA investigations of interactions of a Cycloplatinated Thiosemicarbazone as antiparasitic and antitumor agents with C20 nano-cage. *Int. J. Nano Dimens.*, 2023; 14(3): 219-226.

INTRODUCTION

Thiosemicarbazones ligands formed various complexes with metals. These molecules have been considered as antiparasitics [1, 2], antitumoral [3-7], antibacterial [8, 9] agents.

Nano-cages have been considered as significance drug delivery systems [10]. The C₂₀ molecule is the smallest fullerene [11] and computational investigations have been provided deep insights its properties [12-22]. A DFT study of the solvent effect, features, structures, together with topologies of the interaction between the C₂₀ Cage and cisplatin has been reported [23].

Significant effects of solvents in various fields of chemistry have been revealed [24-26]. Quantum mechanical researches are helpful to inspect the solvent consequence in the structural and properties of numerous molecules [27, 28]. Many computational reports have been employed to illustration of solvent effects on the structural

and properties of inorganic and organometallic complexes [29-42].

Cycloplatinated thiosemicarbazone complexes from 3, 4-dichloroacetophenone thiosemicarbazone have been prepared [43]. Two complexes of them are indicated in Fig. 1. Computational illustration of Interaction of a cycloplatinated thiosemicarbazone as antitumor and antiparasitic agents with B₁₂N₁₂ nano-Cage has been reported [44].

In this work, the interaction of similar complex (CT) of this category and C₂₀ molecule has been reported (Fig. 2), and the solvent influence on the structure and properties of the complex was exemplified. CT...C₂₀ interaction was illustrated with using energy decomposition analysis (EDA) and extended transition state-natural orbitals for chemical valence (ETS-NOCV). Charge transfer between CT and C₂₀ nano-cage were clarified by the charge decomposition analysis (CDA) method.

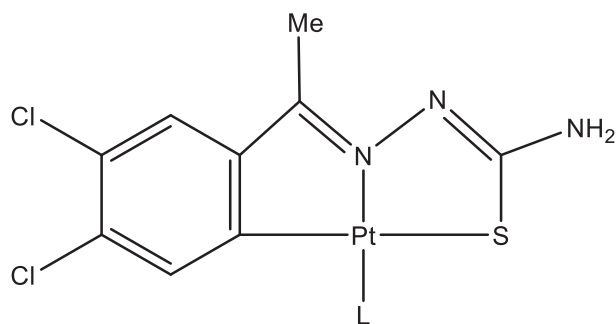
* Corresponding Author Email: rezaghiasi1353@yahoo.com, reza.ghiasi@iaau.ac.ir

Copyright © 2023 The Authors.



This work is licensed under a Creative Commons Attribution-NonCommercial 4.0 International License.,

To view a copy of this license, visit <https://creativecommons.org/licenses/by-nc/4.0/>



L=PPh₃ and 1,3,5-triaza-7-phosphaadamantane

Fig. 1. Structure of two synthesized cycloplatinated thiosemicarbazone complex.

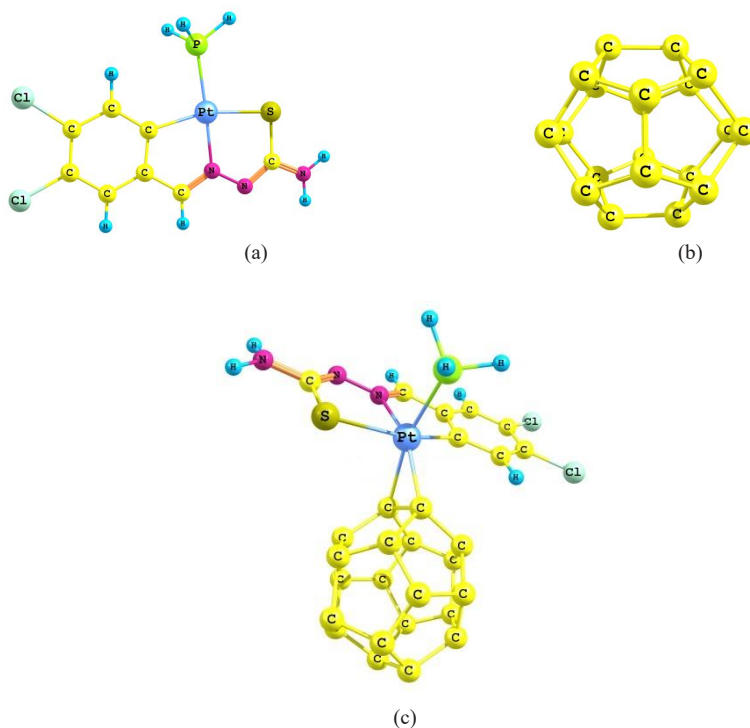


Fig. 2. Structures of (a) studied cycloplatinated thiosemicarbazone complex, (b) C₂₀ nano-cage and (c) optimized structure of studied cycloplatinated thiosemicarbazone (CT) with C₂₀ nano-cage in gas phase.

COMPUTATIONAL METHODS

The studied molecules were optimized using software package of Gaussian 09 [45]. The 6-311G (d, p) [46-49] and the Def2-TZVPPD [50] basis sets were considered for the main group elements and Pt element, respectively. Pseudo-potential effective core potential (ECP) was considered for Pt [51]. The Long range-corrected version of wPBE hybrid function (LC-wPBE) was employed [52-55].

Vibrational analysis conformed that optimized molecules were placed on the minimum potential energy curve. Solution phase calculations were done with Self-consistent reaction field (SCRF) method applying the polarizable continuum model (PCM) [56].

Extended Transition State-Natural Orbitals for Chemical Valence (ETS-NOCV), Independent gradient model (IGMH) analysis [57] and Charge

Table 1. Energy (E, a.u), dipole moment (μ , Debye), solvation energy (ΔE_{solv} , kcal/mol) and interaction energy (ΔE_{int} , kcal/mol) of the complex of studied cycloplatinated thiosemicarbazone (CT) with C_{20} nano-cage in gas and solution phases. ϵ and n are dielectric constant and refractivity index of solvent, respectively.

	ϵ	n	E	μ	ΔE_{solv}	ΔE_{int}
Gas	-		-3013.666	8.82	0.00	-98.52
CF	4.71	1.45	-3013.679	11.92	-8.14	-97.24
DCE	10.13	1.41	-3013.682	12.78	-10.09	-96.86
AC	20.49	1.36	-3013.684	13.25	-11.08	-96.69
PN	29.32	1.366	-3013.684	13.40	-11.39	-96.63
DMF	37.22	1.43	-3013.684	13.47	-11.55	-96.61
DMSO	46.83	1.48	-3013.684	13.54	-11.67	-96.58

decomposition analysis (CDA) [58] were done with Multiwfn 3.8 software package [59]. VMD software was employed to the visualizations of the IGMH result [60].

RESULTS AND DISCUSSION

Energetic aspects

Optimized geometries of C_{20} molecule, CT complex and CT... C_{20} complex are indicated in Fig. 2(a, b, c). Computed energy (E) and solvation energy (DE_{solv}) values of CT... C_{20} complex are listed in Table 1. The CT... C_{20} complex in solution phase has larger stability than gas phase and can be found in the basis of E values. There is more significance stability in more polar solvents. It can be found, smaller DE_{solv} values for more polar solvents. Linear relation between dielectric constant of solvents (ϵ) and DE_{solv} data is:

$$DE_{\text{solv}} = -0.0723 \epsilon - 8.8628; \quad R^2 = 0.7362$$

Considered solvents are: Propanonitrile (PN), chloroform (DF), acetone (AC), dichloroethane (DCE), n,n-dimethylformamide (DMF), and dimethylsulfoxide (DMSO)

Then, the *modified-Buckingham* function ($F_{\text{modified-Buckingham}}$) [61] is considered as equation follow:

$$F_{\text{modified-Buckingham}} = C_1 + C_2 \cdot f(\epsilon) + C_3 \cdot f(n^2) + C_4 \cdot f(\epsilon) \cdot f(n^2)$$

$$f(\epsilon) = \frac{(\epsilon - 1)}{2\epsilon + 1}; \quad f(n^2) = \frac{(n^2 - 1)}{2n^2 + 1}$$

This equation includes the influence of solvent dipolarity ($f(\epsilon)$) and solvent polarizability ($f(n^2)$). Third cross-term considers a mutual relationship in

polarizability/dipolarity variations due to formed solvent/ solute collision complexes in solution.

The relationship between DE_{solv} values and this solvent polarity function is:

$$\Delta E_{\text{solv}} = 12.18 - 49.47 f(\epsilon) - 49.88 f(n^2) + 103.98 f(\epsilon) \cdot f(n^2); \quad R^2 = 0.9999$$

Therefore, it can be found a good correlation between the DE_{solv} values with *modified-Buckingham* function in the studied system.

Interaction energy values

The calculated interaction energy values of the CT... C_{20} complexes are gathered in Table 1. It can be deduced significance interactions between CT and C_{20} nano-cage in solution phase than gas phase. Furthermore, the stronger interaction is observed in more polar solvents. Linear dependence between DE_{int} and ϵ values is:

$$DE_{\text{int}} = 0.0133 \epsilon - 97.098; \quad R^2 = 0.7164$$

The relationship between DE_{int} values and the *modified-Buckingham* function is:

$$\Delta E_{\text{int}} = -97.94 + 2.73 f(\epsilon) - 5.39 f(n^2) + 11.47 f(\epsilon) \cdot f(n^2); \quad R^2 = 0.9999$$

It can be observed a significant relation between the values of the DE_{int} values and *modified-Buckingham* function.

Dipole moment

Computed dipole moment values of the CT... C_{20} complex are shown in Table 1. It can be deduced higher μ values in solution phase than gas phase. Calculated μ values are higher in more polar solvents.

Table 2. $\nu_{\text{sym}}(\text{NH})$ and $\nu_{\text{asym}}(\text{NH})$ values (cm^{-1}) of the complex of studied cycloplatinated thiosemicarbazone with C_{20} nano-cage in gas and solution phases.

	$\nu(\text{N-H})_{\text{sym}}$	$\nu(\text{N-H})_{\text{asym}}$
	3503.00	3635.71
Gas	3663.52	3796.41
CF	3655.47	3785.68
DCE	3654.18	3784.39
AC	3653.48	3783.72
PN	3653.29	3783.55
DMF	3653.21	3783.47
DMSO	3653.16	3783.43

Linear dependence of the values of e and m values is:

$$m = 0.0335 e + 12.228; \quad R^2 = 0.7523$$

The relationship between solvent polarity function and m is:

$$\mu = -1.99 + 32.22 f(\epsilon) + 44.68 f(n^2) - 92.99$$

$$f(\epsilon).f(n^2); \quad R^2 = 0.9999$$

Thus, it can be seen good relationship between the m with *modified-Buckingham* function in the studied system.

Vibrational spectrum analysis

The vibrational analysis of $\text{CT} \dots \text{C}_{20}$ complexes reveal that that the maximum wavenumber values of this complex is due to the asymmetric and symmetric stretching vibration modes of amine ligands. Computed $\nu_{\text{sym}}(\text{NH})$ and $\nu_{\text{asym}}(\text{NH})$ values are gathered in Table 2. These values are larger in solution phase than gas phase. Larger values are found in less polar solvents.

The induced stretching frequency shifts was provided by *modified-Buckingham* function as follows:

$$\frac{(\nu_{\text{solution}} - \nu_{\text{gas}})}{\nu_{\text{gas}}} = \frac{\Delta\nu}{\nu_{\text{gas}}} = C_1 + C_2.f(\epsilon) + C_3.f(n^2) + C_4.f(\epsilon).f(n^2)$$

It can be provided good linear correlation between solvent-induced stretching vibrational frequency shifts of $\nu(\text{NH})$ with the *modified-Buckingham* function:

$$\Delta\nu/\nu_{\text{gas}} = 1.75 \times 10^{-3} - 9.68 \times 10^{-3} f(\epsilon) - 1.03 \times 10^{-2} f(n^2) + 2.24 \times 10^{-2} f(\epsilon).f(n^2); \quad R^2 = 0.9999$$

Molecular orbital analysis

Plots of frontier orbitals of the $\text{C}_{20} \dots \text{CT}$ complexes are presented in Fig. 3 in the gas phase. It can be deduced, C_{20} fragment includes most contributions in HOMO and LUMO. Comparison of the frontier orbital energy values in the CT and $\text{C}_{20} \dots \text{CT}$ complex indicates CT interaction with C_{20} importantly destabilizes and stabilizes the HOMO and LUMO levels of CT, respectively. In addition, HOMO-LUMO gap value is larger in $\text{C}_{20} \dots \text{CT}$ complex than CT. Therefore, we believe that the C_{20} may be a suitable nanoscale carrier for CT drug.

ETS-NOCV method

The Extended Transition State - Natural Orbitals for Chemical Valence (ETS-NOCV) method [62] is defined a mixture of the NOCV method [63] and the ETS approach [64].

ETS-NOCV outcomes reveal that NOCV pair 1 is the main contributor to the DE_{orb} (-328.25 kcal/mol). Computed NOCV pair 1 energy value is -161.94 kcal/mol. The Fig. 4 displays the isosurface of NOCV pair density pair 1. Enhanced and reduced and the electron density are presented with green and blue isosurfaces, respectively, owing to the orbital interaction defined by NOCV pair 1. Obviously, the NOCV pair 1 attributes to important electron shift from the CT fragment to the C_{20} nano-cage. 1.05482 electron is moved electron to this NOCV pair.

IGMH analysis

The interaction of $\text{CT} \dots \text{C}_{20}$ is evaluated with independent gradient model (IGM) based on Hirshfeld partition of molecular density (IGMH) (Fig. 5). It can be detected the Pt..C interactions

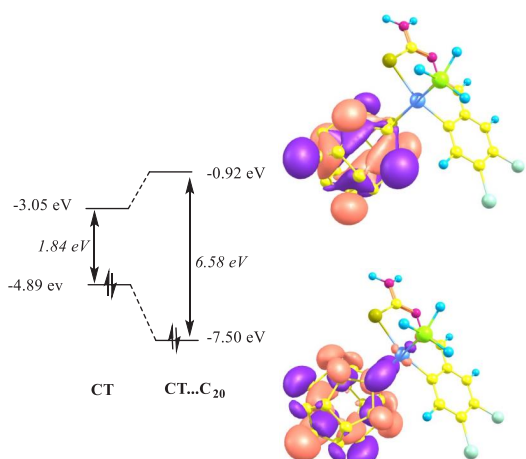
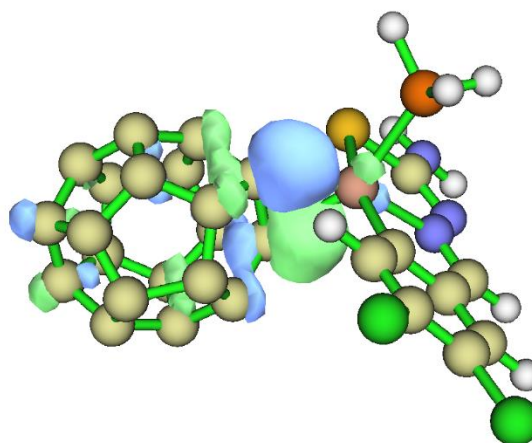
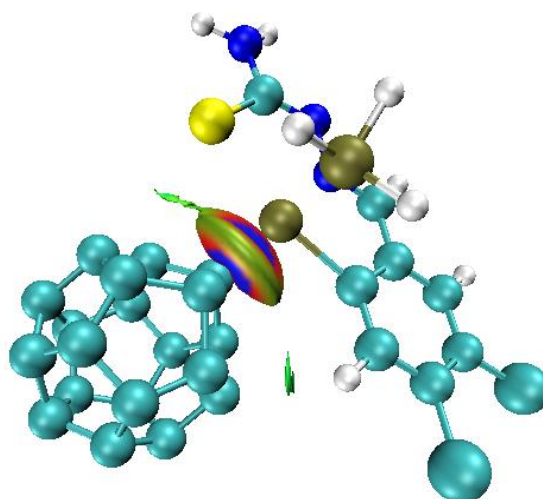


Fig. 3. Plots of frontier orbitals C20...CT complex in gas phase.

Fig. 4. Isosurface of NOCV pair density pair 1 of CT...C₂₀ complex.Fig. 5. Independent gradient model (IGM) based on Hirshfeld partition of molecular density (IGMH) of CT...C₂₀ complex.

(blue color), nearby the middle of the isosurface.

CDA

The charge decomposition analysis (CDA) theory is beneficial approaches to afford significant intuition into the electron transfer. The CDA outcomes display orbital 131 leads 0.017229 electrons donate from C₂₀ cage to CT complex. On the other hand, 0.021980 electrons detached from overlap area between C₂₀ cage and CT. Orbital 88 has small contribution to electron donation (0.037670 electron). Fig. 6 displays isosurfaces of orbital 88 and 131. Also, extended charge decomposition analysis (ECDA) shows that 0.5875 electrons moved from fragment CT complex to C₂₀ cage.

CONCLUSION

In this work, we reported the interaction of a cycloplatinated thiosemicarbazone (CT) as antitumor and antiparasitic agents with C₂₀ molecule. Our calculations revealed the CT...C₂₀ interaction increases in solution than gas phase. The more significance interaction was found in more polar solvents. Smaller polarity was deduced in gas phase than solution phase. The vibrational analysis revealed the maximum wavenumber values of the investigated complex were belonged to the asymmetric and symmetric stretching vibration modes of amine ligands (u(N-H)). Significance relationships were provided between m , DE_{solv} , DE_{int} and u(N-H) data with *modified-Buckingham* function in the CT...C₂₀ systems. ETS-

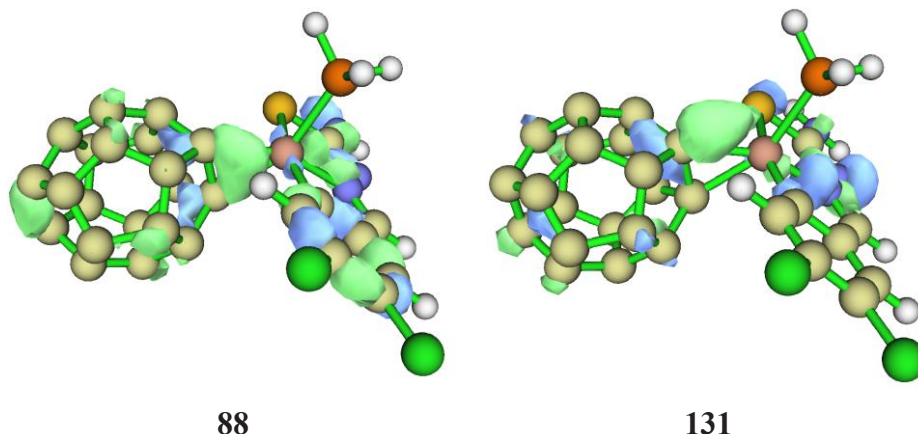


Fig. 6. Isosurfaces of orbitals 88 and 131 of CT...C₂₀ complex.

NOCV outcomes illustrated NOCV pair 1 was the highest subscriber to the DE_{orb} (-328.25 kcal/mol). NOCV pair 1 energy value of the CT...C₂₀ system was -161.94 kcal/mol. CDA findings illustrated electrons donate from CT complex to C₂₀ molecule.

CONFLICTS OF INTEREST

The authors do not have any conflicts of interest.

REFERENCES

- Moreno-Rodríguez A., Salazar-Schettino P. M., Bautista J. L., Hernández-Luis F., Torrens H., Guevara-Gómez Y., Pina-Canseco S., Torres M. B., Cabrera-Bravo M., Martínez C. M., Pérez-Campos E., (2014), In vitro antiparasitic activity of new thiosemicarbazones in strains of *Trypanosoma cruzi*. *Europ. J. Medic. Chem.* 87: 23-29. <https://doi.org/10.1016/j.ejmech.2014.09.027>
- Adams M., Kock C. D., Smith P. J., Land K. M., Liu N., Hopper M., Hsiao A., Burgoyne A. R., Stringer T., Meyer M., Wiesner L., Chibalea K., Smith G. S., (2015), Improved antiparasitic activity by incorporation of organosilane entities into half-sandwich ruthenium(II) and rhodium(III) thiosemicarbazone complexes. *Dalton Trans.* 44:2456-2461. <https://doi.org/10.1039/C4DT03234A>
- Singh N. K., Kumbhar A. A., Pokharel Y. R., Yadav P. N., (2020), Anticancer potency of copper (II) complexes of thiosemicarbazones. *J. Inorg. Biochem.* 210: 111134. <https://doi.org/10.1016/j.jinorgbio.2020.111134>
- Pósa V., Hajdu B., Tóth G., Dömötör O., Kowol C. R., Keppler B. K., Spengler G., Gyurcsik B., Enyedy É. A., (2022), The coordination modes of (thio)semicarbazone copper(II) complexes strongly modulate the solution chemical properties and mechanism of anticancer activity. *J. Inorg. Biochem.* 231: 111786. <https://doi.org/10.1016/j.jinorgbio.2022.111786>
- Lobana T. S., Kaushal M., Bala R., Nim L., Paul K., Arora D. S., Bhatia A., Arora S., Jasinski J. P., (2020), Di-2-pyridylketone-N1-substituted thiosemicarbazone derivatives of copper(II): Biosafe antimicrobial potential and high anticancer activity against immortalized L6 rat skeletal muscle cells. *J. Inorg. Biochem.* 212: 111205. <https://doi.org/10.1016/j.jinorgbio.2020.111205>
- González-Barcia L. M., Fernández-Fariña S., Rodríguez-Silva L., Bermejo M. R., González-Noya A. M., Pedrido R., (2020), Comparative study of the antitumoral activity of phosphine-thiosemicarbazone gold(I) complexes obtained by different methodologies. *J. Inorg. Biochem.* 203: 110931. <https://doi.org/10.1016/j.jinorgbio.2019.110931>
- Cao W., Qi J., Qian K., Tian L., Cheng Z., Wang Y., (2019), Structure-activity relationships of 2quinolinecarboxaldehyde thiosemicarbazone gallium (III) complexes with potent and selective anticancer activity. *J. Inorg. Biochem.* 191: 174-182. <https://doi.org/10.1016/j.jinorgbio.2018.11.017>
- Bisceglie F., Bacci C., Vismarra A., Barilli E., Pioli M., Orsoni N., Pelosi G., (2020), Antibacterial activity of metal complexes based on cinnamaldehyde thiosemicarbazone analogues. *J. Inorg. Biochem.* 203: 110888. <https://doi.org/10.1016/j.jinorgbio.2019.110888>
- Eissa S. I., Farrag A. M., Abbas S. Y., El Shehry M. F., Ragab A., Fayed E. A., Ammar Y. A., (2021), Novel structural hybrids of quinoline and thiazole moieties: Synthesis and evaluation of antibacterial and antifungal activities with molecular modeling studies. *Bioorg. Chem.* 110: 104803. <https://doi.org/10.1016/j.bioorg.2021.104803>
- Ghanbari H., Cousins B. G., Seifalian A. M., (2011), A nanocage for nanomedicine: Polyhedral oligomeric silsesquioxane (POSS). *Macromol. Rapid Commun.* 32: 1032-1046. <https://doi.org/10.1002/marc.201100126>
- Prinzbach H., Weiler A., Landenberger P., Wahl F., Worth J., Scott L. T., Gelmont M. D., Olevano D., Issendorff B. V., (2000), Gas-phase production and photoelectron spectroscopy of the smallest fullerene C₂₀. *Nature.* 407: 60-63. <https://doi.org/10.1038/35024037>
- Chen Z., Heine T., Jiao H., Hirsch A., Thiel W., Schleyer P. V. R., (2004), Theoretical studies on the smallest fullerene: From monomer to oligomers and solid states. *Chem. Eur. J.* 10: 963-970. <https://doi.org/10.1002/chem.200305538>
- Luo J., Peng L. M., Xue Z. Q., Wu J. L., (2004), Positive electron affinity of fullerenes: Its effect and origin. *J. Chem. Phys.* 120: 7998-8001. <https://doi.org/10.1063/1.1691397>

- 14 Shahzad H., Ahmadi R., Adhami F., Najafpour J., (2020), Adsorption of cytarabine on the surface of fullerene C₂₀: A comprehensive DFT study. *Euras. Chem. Communic.* 2: 162-169. <https://doi.org/10.33945/SAMI/ECC.2020.2.1>
- 15 Ahmadi R., (2018), Investigating the effect of fullerene (C₂₀) substitution on the structural and energetic properties of Tetryl by density functional theory. *J. Phys. Theoret. Chem.* 15: 15-25.
- 16 Moghaddam T. S. N., Nikmaram F. R., Ahmadi R., (2017), Density functional theory study of the Behavior of Carbon Nano cone, BP Nano cone and CSi Nano cone as Nano Carriers for 5-fluorouracil anticancer drug in water. *Int. J. New Chem.* 4: 72-77.
- 17 Ghiasi R., Fashami M. Z., Hakimioun A. H., (2014), A density functional approach toward structural features and properties of C₂₀N₂X₂ (X = H, F, Cl, Br, Me) molecules. *J. Theoret. Comput. Chem.* 13: 1450023. <https://doi.org/10.1142/S0219633614500230>
- 18 Alavi H., Ghiasi R., Ghazanfari D., Akhgar M. R., (2014), Interaction of Fe(CO)₄ with C₂₀ cage in gas and solution phases: A theoretical study. *Revue Roumaine de Chimie.* 59: 883-891.
- 19 Alavi H., Ghiasi R., (2017), A theoretical study of the solvent effect on the interaction of C₂₀ and N₂H₂. *J. Struct. Chem.* 58: 30-37. <https://doi.org/10.1134/S002247661701005X>
- 20 Ghiasi R., Sadeghi N., (2017), Evolution of the interaction between C₂₀ cage and Cr(CO)₅: A solvent effect, QTAIM and EDA investigation. *J. Theoret. Comput. Chem.* 16: 1750007. <https://doi.org/10.1142/S0219633617500079>
- 21 Kazemi Z., Ghiasi R., Jamehbozorgi S., (2019), A theoretical study of the influence of solvent polarity on the structure and spectral properties in the interaction of C₂₀ and Si₂H₂. *J. Nanoanal.* 6: 121-128.
- 22 Ghiasi R., Rahimi M., Ahmadi R., (2021), Quantum-chemical investigation into the complexation of titanocene dichloride with C₂₀ and M@C₂₀ (M+= Li, Na, K) cages. *J. Struct. Chem.* 61: 1681-1690. <https://doi.org/10.1134/S0022476620110025>
- 23 Kazemi Z., Ghiasi R., Jamehbozorgi S., (2018), Analysis of the interaction between the C₂₀ cage and cis-PtCl₂(NH₃)₂: A DFT investigation of the solvent effect, structures, properties, and topologies. *J. Struct. Chem.* 59: 1044-1051. <https://doi.org/10.1134/S0022476618050050>
- 24 Selvarengan P., Kolandaivel P., (2002), Studies of solvent effects on conformers of glycine molecule. *J. Mol. Struct: THEOCHEM.* 617: 99-106. [https://doi.org/10.1016/S0166-1280\(02\)00421-9](https://doi.org/10.1016/S0166-1280(02)00421-9)
- 25 Allin S. B., Leslie T. M., Lumpkin R. S., (1996), Solvent effects in molecular hyperpolarizability calculations. *Chem. Mater.* 8: 428-432. <https://doi.org/10.1021/cm950362j>
- 26 Aquino A. J. A., Tunega D., Haberhauer G., Gerzabek M. H., Lischka H., (2002), Solvent effects on hydrogen bonds: A theoretical study. *J. Phys. Chem. A.* 106: 1862-1871. <https://doi.org/10.1021/jp013677x>
- 27 Tomasi J., Mennucci B., Cammi R., (2005), Quantum mechanical continuum solvation models. *Chem. Rev.* 105: 2999-3094. <https://doi.org/10.1021/cr9904009>
- 28 Springborg M., Specialist Periodical Reports: Chemical Modelling, Applications and Theory. Royal Society of Chemistry: Cambridge, UK, 2008; Vol. 5.
- 29 Li Y.-K., Wu H.-Y., Zhu Q., Fu K.-X., Li X.-Y., (2011), Solvent effect on the UV/Vis absorption spectra in aqueous solution: The nonequilibrium polarization with an explicit representation of the solvent environment. *Comput. Theoret. Chem.* 971: 65-72. <https://doi.org/10.1016/j.comptc.2011.06.003>
- 30 Ouennoughi Y., Karce H. E., Aggoun D., Lanez T., Morallon E., (2017), A novel ferrocenic copper (II) complex Salen-like, derived from 5-chloromethyl-2-hydroxyacetophenone and N-ferrocenmethylamine: Design, spectral approach and solvent effect towards electrochemical behavior of Fc⁺/Fc redox couple. *J. Organom. Chem.* 848: 344-351. <https://doi.org/10.1016/j.jorganchem.2017.08.016>
- 31 Aydin M., Akins D. L., (2018), DFT studies on solvent dependence of electronic absorption spectra of free-base and protonated porphyrin. *Computat. Theoret. Chem.* 1132: 12-22. <https://doi.org/10.1016/j.comptc.2018.04.004>
- 32 Wu C.-l., Zhang S.-h., Gou R.-j., Ren F.-d., Zhu S.-f., (2018), Theoretical insight into the effect of solvent polarity on the formation and morphology of 2, 4, 6, 8, 10, 12-hexanitrohexaazaisowurtzitane (CL-20)/2, 4, 6-Trinitro-Toluene (TNT) cocrystal explosive. *Computat. Theoret. Chem.* 1127: 22-30. <https://doi.org/10.1016/j.comptc.2018.02.007>
- 33 Dos Santos H. F., Chagas M. A., De Souza L. A., Rocha W. R., De Almeida M. V., Anconi C. P. A., De Almeida W. B., (2017), Water solvent effect on theoretical evaluation of ¹H-NMR chemical shifts: O-Methyl-Inositol isomer. *J. Phys. Chem. A.* 121: 2839-2846. <https://doi.org/10.1021/acs.jpca.7b01067>
- 34 Ganesan M., Vedamanickam N., Paranthaman S., (2018), Studies of intramolecular H-bond interactions and solvent effects in the conformers of glycolic acid - A quantum chemical study. *J. Theoret. Computat. Chem.* 17: 1850009. <https://doi.org/10.1142/S0219633618500098>
- 35 Shen D., Su P., Wu W., (2018), What kind of neutral halogen bonds can be modulated by solvent effects? *Phys. Chem. Chem. Phys.* 20: 26126-26139. <https://doi.org/10.1039/C8CP05358H>
- 36 Bi T.-J., Xu L.-K., Wang F., Li X.-Y., (2018), Solvent effects for vertical absorption and emission processes in solution using a self-consistent state specific method based on constrained equilibrium thermodynamics. *Phys. Chem. Chem. Phys.* 20: 13178-13190. <https://doi.org/10.1039/C8CP00930A>
- 37 Milani N. N., Ghiasi R., Forghaniha A., (2020), The impact of solvent polarity on the stability, electronic properties and ¹H NMR chemical shift of the conformers of 2-chloro-3-methylcyclohexan-1-one oxime: A conceptual DFT approach. *J. Appl. Spectros.* 86: 1123-1131. <https://doi.org/10.1007/s10812-020-00949-9>
- 38 Kamrava S., Ghiasi R., Marjani A., (2021), The conductor-like polarizable continuum model (CPCM) study of Indenyl effect on ligand substitution reaction in the (h⁵-C₉H₇)Co(CO)₂ complex. *Int. J. Chem. Kinet.* 53: 901-912. <https://doi.org/10.1002/kin.21491>
- 39 Parsa P., Ghiasi R., Marjani A., (2021), Unveiling the influence of solvent polarity on structural, electronic properties, and ³¹P NMR parameters of rhenabenzyne complex. *Inorg. Chem. Communic.* 124: 108479. <https://doi.org/10.1016/j.inoche.2021.108479>



- 40 Kamrava S., Ghiasi R., Marjani A., (2021), Structure, electronic properties and slippage of cyclopentadienyl and indenyl ligands in the (h5-C5H5) (h3-C5H5) W(CO)2 and (h5-C9H7) (h3-C9H7)W(CO)2 complexes: A C-PCM investigation. *J. Molec. Liq.* 329: 115535. <https://doi.org/10.1016/j.molliq.2021.115535>
- 41 Ghiasi R., Emami R., Sofiyani M. V., (2021), Cyclometalation in the (h3-C5H5)Co(h2-C2H2)(PMe3) and (h3-C9H7)Co(h2-C2H2) (PMe3) complexes: A computational investigation. *J. Molec. Liq.* 325: 115097. <https://doi.org/10.1016/j.molliq.2020.115097>
- 42 Ghiasi R., Milani N. N., (2021), Exploring of the solvent effect on the electronic structure and 14N NMR chemical shift of cyclic-N3S3Cl3: A computational investigation. *Russ. J. Phys. Chem. B.* 15: S14-S21. <https://doi.org/10.1134/S1990793121090086>
- 43 Chellan P., Land K. M., Shokar A., Au A., An S. H., Clavel C. M., Dyson P. J., Kock C. D., Smith P. J., Chibale K., Smith G. S., (2012), Exploring the versatility of cycloplatinated thiosemicarbazones as antitumor and antiparasitic agents. *Organomet.* 31: 5791-5799. <https://doi.org/10.1021/om300334z>
- 44 Ghiasi R., Valizadeh A., (2023), Computational investigation of interaction of a cycloplatinated thiosemicarbazone as antitumor and antiparasitic agents with B12N12 nano-cage. *Res. Chem.* 5: 100768. <https://doi.org/10.1016/j.rechem.2023.100768>
- 45 Frisch M. J., Trucks G. W., Schlegel H. B., Scuseria G. E., Robb M. A., Cheeseman J. R., Scalmani G., Barone V., Mennucci B., Petersson G. A., Nakatsuji H., Caricato M., Li X., Hratchian H. P., Izmaylov A. F., Bloino J., Zheng G., Sonnenberg J. L., Hada M., Ehara M., Toyota K., Fukuda R., Hasegawa J., Ishida M., Nakajima T., Honda Y., Kitao O., Nakai H., Vreven T., J. A. Montgomery J., Peralta J. E., Ogliaro F., Bearpark M., Heyd J. J., Brothers E., Kudin K. N., Staroverov V. N., Keith T., Kobayashi R., Normand J., Raghavachari K., Rendell A., Burant J. C., Iyengar S. S., Tomasi J., Cossi M., Rega N., Millam J. M., Klene M., Knox J. E., Cross J. B., Bakken V., Adamo C., Jaramillo J., Gomperts R., Stratmann R. E., Yazyev O., Austin A. J., Cammi R., Pomelli C., Ochterski J. W., Martin R. L., Morokuma K., Zakrzewski V. G., Voth G. A., Salvador P., Dannenberg J. J., Dapprich S., Daniels A. D., Farkas O., Foresman J. B., Ortiz J. V., Cioslowski J., Fox D. J. *Gaussian 09, Revision D.01*; Gaussian, Inc.: Wallingford CT, 2013.
- 46 Hay P. J., (1977), Basis sets for molecular calculations - representation of 3D orbitals in transition-metal atoms. *J. Chem. Phys.* 66: 4377-4384. <https://doi.org/10.1063/1.433731>
- 47 Krishnan R., Binkley J. S., Seeger R., Pople J. A., (1980), Self consistent molecular orbital methods. XX. A basis set for correlated wave functions. *J. Chem. Phys.* 72: 650-654. <https://doi.org/10.1063/1.438955>
- 48 McLean A. D., Chandler G. S., (1980), Contracted gaussian-basis sets for molecular calculations. 1. 2nd row atoms, Z=11-18. *J. Chem. Phys.* 72: 5639-5648. <https://doi.org/10.1063/1.438980>
- 49 Wachters A. J. H., (1970), Gaussian basis set for molecular wavefunctions containing third-row atoms. *J. Chem. Phys.* 52: 1033-1036. <https://doi.org/10.1063/1.1673095>
- 50 Rappoport D., Furche F., (2010), Property-optimized gaussian basis sets for molecular response calculations. *J. Chem. Phys.* 133: 134105 <https://doi.org/10.1063/1.3484283>
- 51 Andrae D., Haeussermann U., Dolg M., Stoll H., Preuss H., (1990), Energy-adjusted ab initio pseudopotentials for the 2nd and 3rd row transition-elements. *Theor. Chim. Acta.* 77: 123-141. <https://doi.org/10.1007/BF01114537>
- 52 Vydrov O. A., Scuseria G. E., Perdew J. P., (2007), Tests of functionals for systems with fractional electron number. *J. Chem. Phys.* 126: 154109. <https://doi.org/10.1063/1.2723119>
- 53 Vydrov O. A., Scuseria G. E., (2006), Assessment of a long range corrected hybrid functional. *J. Chem. Phys.* 125: 234109. <https://doi.org/10.1063/1.2409292>
- 54 Tawada Y., Tsuneda T., Yanagisawa S., Yanai T., Hirao K., (2004), A long-range-corrected time-dependent density functional theory. *J. Chem. Phys.* 120: 8425-8431. <https://doi.org/10.1063/1.1688752>
- 55 Vydrov O. A., Heyd J., Krukau A., Scuseria G. E., (2006), Importance of short-range versus long-range Hartree-Fock exchange for the performance of hybrid density functionals. *J. Chem. Phys.* 125: 074106. <https://doi.org/10.1063/1.2244560>
- 56 Tomasi J., Mennucci B., Cammi R., (2005), Quantum mechanical continuum solvation models. *Chem. Rev.* 105: 2999-3093. <https://doi.org/10.1021/cr9904009>
- 57 Lu T., Chen Q., (2022), Independent gradient model based on Hirshfeld partition: A new method for visual study of interactions in chemical systems. *J. Comput. Chem.* 43: 539-544. <https://doi.org/10.1002/jcc.26812>
- 58 Xiao M., Lu T., (2015), Generalized charge decomposition analysis (GCDA) method. *J. Adv. Phys. Chemistry.* 4: 111-124. <https://doi.org/10.12677/JAPC.2015.44013>
- 59 Lu T., Chen F., (2012), Multiwfn: A Multifunctional Wavefunction Analyzer. *J. Comp. Chem.* 33: 580-592. <https://doi.org/10.1002/jcc.22885>
- 60 Humphrey W., Dalke A., Schulten K., (1996), VMD-Visual molecular dynamics. *J. Mol. Graphics.* 14: 33-38. [https://doi.org/10.1016/0263-7855\(96\)00018-5](https://doi.org/10.1016/0263-7855(96)00018-5)
- 61 Beka'rek V., Mikulecka A., (1978), A note on evaluation of solvent shifts in IR spectroscopy. *Collect. Czech. Chem. Commun.* 43: 2879-2881. <https://doi.org/10.1135/cccc19782879>
- 62 Mitoraj M. P., Michalak A., Ziegler T., (2009), Combined charge and energy decomposition scheme for bond analysis. *Chem. Theory Comput.* 5: 962-975. <https://doi.org/10.1021/ct800503d>
- 63 Michalak A., Mitoraj M., Ziegler T., (2008), Bond orbitals from chemical valence theory. *J. Phys. Chem. A.* 112: 1933-1939. <https://doi.org/10.1021/jp075460u>
- 64 Ziegler T., Rauk A., (1977), On the calculation of bonding energies by the Hartree Fock Slater method. *Theor. Chim. Acta.* 46: 1-10. <https://doi.org/10.1007/BF02401406>

